

Corrective Diffusion Language Models

Shuibai Zhang¹ Fred Zhangzhi Peng² Yiheng Zhang¹ Jin Pan¹ Grigoris G Chrysos¹

Abstract

Diffusion language models are structurally well-suited for iterative error correction, as their non-causal denoising dynamics allow arbitrary positions in a sequence to be revised. However, standard masked diffusion language model (MDLM) training fails to reliably induce this behavior, as models often cannot identify unreliable tokens in a complete input, rendering confidence-guided refinement ineffective. We study *corrective behavior* in diffusion language models, defined as the ability to assign lower confidence to incorrect tokens and iteratively refine them while preserving correct content. We show that this capability is not induced by conventional masked diffusion objectives and propose a correction-oriented post-training principle that explicitly supervises visible incorrect tokens, enabling error-aware confidence and targeted refinement. To evaluate corrective behavior, we introduce the Code Revision Benchmark (CRB), a controllable and executable benchmark for assessing error localization and in-place correction. Experiments on code revision tasks and controlled settings demonstrate that models trained with our approach substantially outperform standard MDLMs in correction scenarios, while also improving pure completion performance. Our code is publicly available at <https://github.com/zhangshuibai/CDLM>.

1. Introduction

Autoregressive (AR) language models have long been the dominant paradigm for text generation by predicting tokens from left to right (Achiam et al., 2023; Guo et al., 2025a; Comanici et al., 2025; Yang et al., 2025; Grattafiori et al., 2024). Recently, diffusion language models (DLMs) have emerged as a structurally distinct alternative, replacing causal generation with an iterative denoising process over complete sequences (Nie et al., 2025; Ye et al., 2025; Labs et al.,

¹University of Wisconsin–Madison ²Duke University. Correspondence to: Shuibai Zhang <shuibai@cs.wisc.edu>.

2025; Song et al., 2025; Zhu et al., 2025). This non-causal formulation decouples token predictions across positions and enables parallel generation (Kang et al., 2025). Beyond differences in sampling efficiency and generation dynamics, this structural distinction endows DLMs with a capability that AR models fundamentally lack: the ability to directly refine an existing sequence through localized, iterative revisions (Wang et al., 2025; Peng et al., 2025a). Because arbitrary positions can be modified without regenerating the entire context, DLMs are naturally suited for correcting errors in place and progressively improving a complete input. In AR models, later predictions are conditioned on earlier outputs, so an error at an early position propagates forward and cannot be corrected without regenerating the remaining sequence. This sequential dependency makes localized revision difficult. In contrast, diffusion language models decouple predictions across positions, enabling targeted refinement beyond left-to-right generation.

Despite this structural advantage, standard masked diffusion language models (MDLMs) do not reliably exhibit effective refinement behavior. Under the conventional masked-diffusion objective, supervision is applied only to masked positions, while incorrect but unmasked tokens receive no gradient signal. This training setup provides little incentive for the model to distinguish between correct and incorrect content or to calibrate confidence in a way that reflects token-level reliability (Ni et al., 2025). As a result, the model offers limited guidance on where edits are needed during iterative refinement. Although prior work has explored combining absorbing noise and uniform noises together to improve generation performance via self-correction, its implications for enabling practical, targeted correction have not been carefully examined (von Rütte et al., 2025). To formalize this gap, we introduce the notion of *corrective behavior*: the ability of a model to identify unreliable tokens in a complete input and iteratively refine them while preserving correct content. This capability is essential for effective refinement but is not induced by standard MDLM training objectives.

A key challenge in studying refinement is the absence of a controlled and executable benchmark that directly evaluates such behavior. Most existing evaluations are built around prefix-based completion, where models generate continuations from a given prefix, a setting tailored to autoregressive models and their left-to-right generation process (Du et al.,

2024; Austin et al., 2021b; Liu et al., 2023b). These evaluations do not assess whether a model can localize and fix errors in a complete input, which is the core requirement of refinement. A suitable refinement benchmark must allow precise control over corruption type and severity and provide reliable feedback on whether a proposed correction is valid. These considerations motivate the development of both an appropriate benchmark and a post-training principle that equips MDLMs with error-aware, targeted refinement capabilities. We refer to MDLMs that exhibit such corrective behavior as *Corrective Diffusion Language Models (CDLMs)*.

Our contributions. In this work, we make the following contributions:

- **A controllable and executable refinement benchmark.** We introduce the **Code Revision Benchmark (CRB)**, constructed by applying type-preserving corruptions of controllable difficulty to real, executable code snippets. CRB enables systematic evaluation of error localization and iterative refinement, with each instance graded through deterministic execution. While our methodology is general, code provides an ideal testbed due to its practical importance and the availability of unambiguous correctness signals.
- **A post-training principle for obtaining Corrective Diffusion Language Models (CDLMs).** We revisit the absorbing-uniform mixture objective from the perspective of targeted correction, and show that it provides the missing supervision needed for masked diffusion language models to recognize incorrect tokens and prioritize edits. By explicitly supervising visible corrupted tokens alongside masked reconstruction, this principle induces error-aware confidence and enables reliable, targeted refinement.
- **Improved pure generation through corrective ability.** CDLMs consistently improve pure completion performance across both code-generation benchmarks and controlled environments such as Sudoku. Compared to standard MDLMs, CDLMs achieve higher completion accuracy. These results suggest that the error-aware confidence calibration induced by correction-oriented training also benefits general denoising-based generation.

2. Background

Masked Diffusion Language Models

Let $\mathbf{x} = (x_1, \dots, x_n)$ be a clean token sequence over a vocabulary \mathcal{V} , and let $m \in \mathcal{V}$ denote a designated absorbing mask token. We focus on *masked diffusion language models*

(MDLMs) (Sahoo et al., 2024), a widely used class of diffusion language models based on an absorbing corruption process (Nie et al., 2025; Ye et al., 2025; Labs et al., 2025; Song et al., 2025; Zhu et al., 2025).

2.1. Forward (noising) process.

For each training example, a mask ratio $\lambda \sim \text{Uniform}[0, 1]$ is sampled, and the corrupted sequence \mathbf{z} is drawn as

$$q_\lambda(\mathbf{z} \mid \mathbf{x}) = \prod_{i=1}^n \begin{cases} \lambda, & z_i = m, \\ 1 - \lambda, & z_i = x_i. \end{cases}$$

Reverse (denoising) model. A Transformer parameterizes the conditional distribution $p_\theta(\mathbf{x} \mid \mathbf{z})$ and is trained using a masked-token reconstruction objective,

$$\mathcal{L}_{\text{absorb}}(\theta) = \mathbb{E}_{\mathbf{x} \sim \mathcal{D}, \mathbf{z} \sim q_\lambda(\cdot \mid \mathbf{x})} \left[- \sum_{i: z_i = m} \log p_\theta(x_i \mid \mathbf{z}) \right].$$

Only positions with $z_i = m$ contribute to the loss, while logits at all non-masked positions are ignored. As illustrated in Figure 2, although the model produces logits for every position in the sequence, gradients are backpropagated exclusively through masked locations. Consequently, the model is never explicitly trained to assign different confidence to *correct* versus *incorrect* unmasked tokens.

2.2. Confidence-Based Iterative Refinement

Diffusion language models refine sequences by iteratively predicting token-level distributions and selectively remasking uncertain positions (Peng et al., 2025a; Wang et al., 2025; Kim et al., 2025). Given the current sequence $\mathbf{z}^{(t)}$, the model produces a conditional token-level distribution $p_\theta(\cdot \mid \mathbf{z}^{(t)})$. From this distribution, we extract both the token prediction and its associated confidence:

$$\hat{x}_i^{(t)} = \arg \max_{v \in \mathcal{V}} p_\theta(v \mid \mathbf{z}^{(t)}), \quad c_i^{(t)} = \max_{v \in \mathcal{V}} p_\theta(v \mid \mathbf{z}^{(t)}).$$

Confidence-based refinement then identifies positions whose confidence falls below a predefined threshold τ ,

$$r^{(t)} = \{ i \mid c_i^{(t)} < \tau \},$$

and constructs the next iteration via a unified update rule:

$$z_i^{(t+1)} = \begin{cases} m, & i \in r^{(t)}, \\ \hat{x}_i^{(t)}, & \text{otherwise.} \end{cases}$$

This approach aims to focus edits on positions deemed unreliable by the model. However, in practice, token-level confidence in diffusion language models is often poorly aligned with correctness (Figure 2), causing threshold-based refinement to either miss genuine errors or unnecessarily remask correct tokens, and thereby making targeted error correction unreliable.

3. Related Work

Development of Diffusion Language Models The development of diffusion-based language modeling begins with continuous-space approaches such as DiffusionLM (Li et al., 2022), which apply Gaussian noise in continuous space over token embeddings but remain misaligned with the discrete nature of textual data. The introduction of D3PM (Austin et al., 2021a) establishes a unified framework for discrete-state diffusion through flexible transition kernels, encompassing uniform, absorbing, and structured corruption processes. Exploration of uniform-noise discrete diffusion, exemplified by Schiff et al. (2025), demonstrates limited suitability for natural language due to excessive semantic destruction. Absorbing-noise diffusion subsequently emerges as a more stable alternative for text. Diffusion-BERT (He et al., 2023) shows that using a single absorbing token (e.g., [MASK]) significantly improves training dynamics and sample quality. Building on these developments, the masked diffusion language model (MDLM) formulation (Sahoo et al., 2024) interprets masked diffusion as a variational objective composed of weighted masked language modeling (MLM)-style reconstruction terms and achieves strong performance among discrete diffusion language models. Systematic scaling studies (Ni et al., 2025; Nie et al., 2025) further confirm that MDLM can outperform autoregressive models when scaling up.

Self-correction in Diffusion Language Models. Recent work has shown that diffusion language models may accumulate errors during parallel decoding. Kang et al. (2025) and Chen et al. (2025) demonstrate that parallel denoising steps can introduce or amplify token-level inconsistencies, highlighting the need for mechanisms that explicitly identify and correct decoding errors. A number of subsequent approaches address this issue by incorporating remasking strategies or auxiliary guidance during inference. Peng et al. (2025a) propose a remask-based decoding procedure that relies on an external planner to select tokens for resampling, while Wang et al. (2025) introduce remasking discrete diffusion models that guide inference-time remasking using token-level confidence to improve generation quality without additional training. Similarly, Lee et al. (2025a) employ an auxiliary scoring model to assess intermediate predictions and determine whether remasking is necessary. Kim et al. (2025) further integrate remasking decisions into the model itself by introducing an internal prediction head that estimates, for each token, the probability that it should be remasked, enabling model-internal correction without external supervision. Most relevant to our work, von Rütte et al. (2025) propose the Generalized Interpolating Discrete Diffusion framework, which combines absorbing and uniform noise to generalize discrete diffusion and improve generation quality. Despite similarities in noise design, this

framework differs fundamentally in its sampling mechanism: it performs holistic diffusion updates in which all token positions may change across denoising steps. In contrast, our approach follows the masked diffusion paradigm, in which decoding explicitly restricts updates to masked or remasked positions.

4. Code Revision Benchmark (CRB)

Both autoregressive and diffusion language models are commonly evaluated through prefix-based completion (Nie et al., 2025; Song et al., 2025; Ni et al., 2025), which does not assess their ability to localize and correct errors in a complete input sequence. A systematic evaluation of refinement behavior instead requires controlled variation of error types, fine-grained control over corruption severity, and deterministic verification of correctness. Code provides an ideal testbed for such evaluation, as program behavior is executable and correctness can be checked deterministically. Building on widely used code-generation benchmarks, including HumanEval (Chen et al., 2021) and MBPP (Austin et al., 2021b) and their extended variants HumanEval+ and MBPP+ (Liu et al., 2023a), we introduce the *Code Revision Benchmark (CRB)*. CRB leverages these established datasets while introducing controlled, localized corruptions to enable systematic analysis of error localization and iterative, in-place correction.

4.1. Task Definition

Let $\mathbf{x}^* = (x_1^*, \dots, x_n^*)$ denote a canonical program represented as a sequence of n tokens drawn from a vocabulary \mathcal{V} . CRB introduces errors by selecting an index set $E \subseteq \{1, \dots, n\}$ and applying a type-preserving replacement operator,

$$z_i^{(0)} = \begin{cases} \phi(x_i^*), & i \in E, \\ x_i^*, & \text{otherwise.} \end{cases}$$

The operator $\phi(\cdot)$ replaces a token with another token from the same lexical category while preserving token length under the tokenizer. This design avoids trivial surface-level cues for error detection and yields realistic syntactic or semantic faults that require targeted, in-place correction (Wang & Zhao, 2024; Xu & Sheng, 2024).

4.2. Corruption Types

CRB includes three categories of token-level corruption:

- **Operator substitutions.** An operator token is replaced using a predefined set $\mathcal{O} = \{+, -, *, /, \%, <, >, <=, >=, ==, !=\}$. These substitutions typically alter program logic or control flow.
- **Identifier substitutions.** A token belonging to the

identifier class is replaced with another identifier that appears within the same scope of the program. This class includes variable names, function names, and language-defined identifiers such as `True` or `False`. Such substitutions often induce subtle semantic inconsistencies.

- **Literal substitutions.** Numeric or boolean literals are replaced with others of the same type, introducing incorrect boundary conditions or erroneous behaviors.

4.3. Difficulty Control via Number of Replacements

The corruption severity is controlled by the number of modified positions $|E|$. The case $|E| = 1$ corresponds to a single-error setting with a localized refinement target. Larger values $|E| > 1$ create multi-error scenarios that require coordinated edits and expose the model’s ability to perform multi-step correction. This explicit control over difficulty is essential for analyzing refinement behavior across progressively challenging settings.

4.4. Executable Validation and Instance Construction

Not all type-preserving corruptions necessarily introduce actual errors: in some cases, a modified program may remain semantically correct and pass all tests. To ensure that every CRB instance contains a genuine syntactic or semantic fault with deterministic supervision, we perform executable validation after corruption. Following corruption, the modified program $z^{(0)}$ is executed using a deterministic grader:

$$\text{Tests}(z^{(0)}) = \begin{cases} \text{pass,} & \text{discard the sample,} \\ \text{fail,} & \text{accept as a CRB instance.} \end{cases}$$

Only programs that fail the tests are retained. This procedure guarantees that every CRB instance contains an actual syntactic or semantic error. The resulting dataset provides controlled, type-preserving corruptions together with deterministic correctness signals, enabling reliable evaluation of both error localization and iterative refinement.

5. Corrective Behavior in Conventional Diffusion Language Models

To characterize the *corrective behavior* of existing diffusion language models on code error correction, we evaluate several publicly available DLMs on CRB, including LLaDA-8B-Base (Nie et al., 2025), Dream-7B-Base (Ye et al., 2025), and Open-dCoder-0.5B (Peng et al., 2025b). Our analysis focuses on two complementary aspects of corrective behavior: (i) the ability to identify erroneous tokens within a complete input, and (ii) the ability to correct such errors through iterative, in-place refinement. All evaluations follow each model’s standard masked-diffusion decoding

HumanEval/31 Canonical Solution:

```

def is_prime(n):
    """Return true if a given number is prime,
    and false otherwise."""
    if n < 2:
        return False
    for k in range(2, n - 1):
        if n % k == 0:
            return False
    return True

Operator: if n % k == 0           if n - k == 0
Identifier: return False         return True
Literal: if n < 2:               if n < 0:

```

Figure 1. CRB corruption pipeline. A canonical program is tokenized, corrupted via type-preserving token replacement, validated by execution, categorized, and generated as a benchmark instance.

procedure, using the confidence-threshold-based refinement described in Section 2.2. Models are tested across multiple difficulty levels by varying both the number of corrupted tokens $|E|$ and the error type.

5.1. Error-Token Identification Performance

We first evaluate whether diffusion language models can identify erroneous tokens based on their token-level confidence scores at the initial refinement step. Given a corrupted program with error positions $E \subseteq \{1, \dots, n\}$, the model assigns each position a confidence score

$$c_i = \max_{v \in \mathcal{V}} p_\theta(v \mid \mathbf{x}),$$

and we examine how well these scores align with the presence of errors. We report two complementary metrics that capture different aspects of error-token identification.

Confidence Gap. The confidence gap measures the average difference between confidence assigned to clean positions and that assigned to erroneous positions:

$$\text{Gap} = \mathbb{E}_{i \notin E}[c_i] - \mathbb{E}_{i \in E}[c_i].$$

A larger positive gap indicates that the model assigns systematically lower confidence to erroneous tokens than to clean ones. This metric reflects the degree to which the model’s confidence is calibrated with respect to token-level correctness.

Top- K Hit Rate. For a fixed K , the Top- K set consists of the K positions with the lowest confidence scores. The hit rate is defined as

$$\text{Hit}@K = \mathbb{I}(E \cap \text{TopK}(c) \neq \emptyset).$$

This metric measures whether at least one true error is ranked among the most uncertain positions. It captures the

Table 1. Evaluation of confidence quality (top block) and iterative correction performance (bottom block) under varying numbers of corrupted tokens n_{replace} . The top block reports the confidence gap between clean and erroneous tokens (gap), together with top-1 and top-5 hit rates measuring how often error tokens appear among the lowest-confidence positions. The bottom block reports Pass@1 after applying confidence-threshold-based iterative refinement for $T \in \{1, 2, 4\}$ refinement steps.

Model	$n_{\text{replace}} = 1$			$n_{\text{replace}} = 2$			$n_{\text{replace}} = 3$			$n_{\text{replace}} = 4$			$n_{\text{replace}} = 5$		
	gap	top-1	top-5												
Dream-7B-Base	0.578	0.094	0.590	0.536	0.084	0.614	0.528	0.084	0.597	0.528	0.088	0.600	0.529	0.076	0.571
LLaDA-8B-Base	0.235	0.178	0.770	0.209	0.198	0.801	0.199	0.172	0.811	0.185	0.159	0.784	0.191	0.162	0.833
Open-dCoder-0.5B	0.106	0.147	0.509	0.100	0.222	0.655	0.085	0.243	0.701	0.089	0.325	0.759	0.093	0.348	0.795

Model	$n_{\text{replace}} = 1$			$n_{\text{replace}} = 2$			$n_{\text{replace}} = 3$			$n_{\text{replace}} = 4$			$n_{\text{replace}} = 5$		
	T=1	T=2	T=4												
Dream-7B-Base	0.776	0.745	0.732	0.704	0.695	0.686	0.663	0.670	0.673	0.654	0.682	0.683	0.630	0.653	0.644
LLaDA-8B-Base	0.552	0.587	0.596	0.419	0.466	0.483	0.338	0.405	0.421	0.319	0.374	0.407	0.280	0.327	0.359
Open-dCoder-0.5B	0.143	0.230	0.251	0.059	0.162	0.178	0.036	0.116	0.141	0.017	0.089	0.104	0.005	0.061	0.074

model’s ability to prioritize error tokens when refinement is restricted to a small set of candidate locations.

Results. Table 1 summarizes error-token identification performance across increasing corruption severity. Across all models, the confidence gap between clean and erroneous tokens remains limited, with particularly weak separation for Open-dCoder-0.5B. Even under the simplest setting with a single corrupted token, erroneous positions receive confidence values comparable to those of clean tokens. These results indicate that token-level confidence provides only limited separation between correct and incorrect positions.

Top- K hit rates reveal a complementary trend. While Top-1 hit rates remain low across models and corruption levels, Top-5 hit rates are substantially higher, suggesting that erroneous tokens are often assigned relatively lower confidence than clean tokens, but are rarely ranked as the single most uncertain position. This disparity indicates that current masked diffusion language models exhibit a coarse ability to place errors within a broad low-confidence region, yet their confidence signals lack the resolution required for precise error localization. As a result, confidence-based ranking alone is insufficient to reliably identify error tokens, limiting its effectiveness as a foundation for targeted, in-place refinement.

5.2. Error-Correction Ability via Iterative Refinement

We next evaluate whether diffusion language models can repair corrupted programs through iterative, in-place refinement. At each refinement step t , the model selectively remasks a subset of positions and re-predicts their values based on token-level confidence scores. Let $c_i^{(t)}$ denote the confidence assigned to token i after step t .

Iterative Refinement. We follow the confidence-threshold-based refinement protocol introduced in

Section 2.2. Given a fixed threshold τ , all positions whose confidence falls below the threshold are remasked at step t :

$$r^{(t)} = \{ i : c_i^{(t)} < \tau \}.$$

Unless otherwise specified, we set $\tau = 0.9$ in all experiments. This dynamic strategy allows the remasking set to adapt to the model’s evolving uncertainty across refinement steps.

Pass@1 Metric. After T refinement steps, the final program is executed using an external grader. Pass@1 is defined as the fraction of programs that execute successfully and produce the correct output:

$$\text{Pass@1} = \mathbb{I}(\text{grader}(x^{(T)}) = \text{correct}).$$

Results. Table 1 reports Pass@1 after iterative refinement using the confidence-threshold-based strategy. Overall, error-correction performance remains limited across all models and corruption levels, even under the simplest setting with a single corrupted token. Notably, even the strongest model, Dream-7B-Base, fails to correct a substantial fraction of programs, indicating that targeted correction is challenging for standard diffusion language models.

Across models, correction performance follows a consistent ordering, with Dream-7B-Base performing best, followed by LLaDA-8B-Base, and Open-dCoder-0.5B trailing significantly behind. This trend reflects differences in overall modeling capacity (Ye et al., 2025; Peng et al., 2025b), suggesting that limited representational strength further constrains corrective behavior, particularly for smaller models.

Increasing the number of refinement steps yields only marginal and inconsistent improvements. In many cases, additional steps fail to substantially improve Pass@1. This behavior is consistent with the weak error-token identification observed in Section 5.1: because low-confidence

positions do not reliably correspond to true errors, iterative remasking often overwrites correct tokens while leaving actual errors unresolved. As a result, simply applying more refinement steps is unlikely to overcome the limitations imposed by inaccurate error localization.

5.3. Self-revision under minimal corruption

The Code Revision Benchmark (CRB) constructs revision instances by introducing controlled corruptions to canonical programs. While this design isolates error localization and correction behavior, it also raises a potential confound: a model may fail to revise a corrupted program simply because the input falls outside the distribution of code it typically generates. In such cases, poor revision performance could reflect distributional mismatch rather than a genuine inability to detect and correct errors.

To disentangle these factors, we design a *self-revision under minimal corruption* setting, in which each model is evaluated exclusively on programs that it has already demonstrated the ability to generate correctly. By introducing only a minimal, localized perturbation to model-generated solutions, this setting ensures that revision failures cannot be attributed to unfamiliar inputs, and instead directly probe the model’s capacity for targeted error detection and correction.

Setup. For each model, we first identify a set of programs that the model can generate correctly under standard decoding. Starting from these correct model-generated programs, we introduce a single type-preserving token corruption ($n_{\text{replace}} = 1$) using the CRB corruption pipeline. Restricting to a single-token modification ensures that the corrupted program remains extremely close to the model’s own generation distribution, differing from a correct solution only through a minimal and localized perturbation. This design isolates the model’s ability to recognize and revise a small error, rather than its capacity to handle large semantic changes or distributional shifts.

We then apply iterative refinement to the corrupted program and evaluate whether the model can revise it back to a correct solution. Performance is measured using Pass@1 after varying numbers of refinement steps, ranging from 1 to 4.

Results. We evaluate self-revision performance under a single-token corruption setting in Table 2. Even when starting from programs that each model has itself generated and verified as correct, all evaluated diffusion language models achieve relatively low Pass@1 after revision. Increasing the number of refinement steps from 1 to 4 yields only marginal and non-monotonic improvements, indicating that additional iterations do not reliably enhance correction performance. Notably, these failures persist despite the minimal and localized nature of the corruption, and despite

Model	T=1	T=2	T=3	T=4
LLaDA-8B-Base	0.550	0.571	0.577	0.580
Dream-7B-Base	0.528	0.548	0.402	0.427
Open-dCoder-0.5B	0.203	0.342	0.344	0.336

Table 2. Self-revision under minimal corruption on HumanEval.

For each model, we first generate programs and retain only those that pass all tests. A single type-preserving token corruption ($n_{\text{replace}} = 1$) is then applied to each correct program, and the model is evaluated on its ability to revise the corrupted program back to a passing solution using iterative refinement. Reported values correspond to Pass@1 after different numbers of refinement steps.

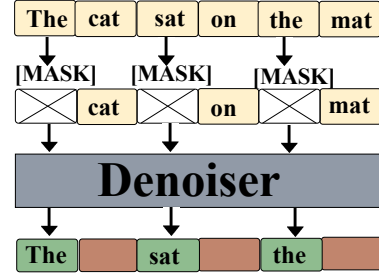


Figure 2. Illustration of absorbing-mask training. Cross-marked boxes denote masked tokens, while beige tokens are visible inputs. Green outputs indicate masked positions where the reconstruction loss is applied, whereas brown outputs correspond to unmasked tokens that receive no supervision during training.

the fact that the original programs lie squarely within each model’s own generation distribution. Together, these results indicate that poor revision performance cannot be attributed to distribution mismatch, but instead reflects fundamental limitations in the models’ corrective behavior.

Discussion. The self-revision experiment reveals a fundamental asymmetry between generation and correction in diffusion language models. Although the models are capable of generating correct programs, they often fail to identify and repair even a single incorrect token once it is introduced. This discrepancy indicates that effective correction requires more than generative competence alone. In particular, it relies on the model’s ability to be aware of its own uncertainty, to distinguish reliable tokens from unreliable ones, and to localize errors for targeted, in-place revision. When these capabilities are weak or absent, iterative refinement becomes unreliable even under minimal corruption. These observations directly motivate the correction-oriented training principle introduced in the next section.

6. Towards Corrective Behavior

Standard masked diffusion language models trained with the absorbing-mask objective often exhibit limited error awareness during refinement. As illustrated in Figure 2, unmasked tokens receive no direct supervision, which limits the model’s ability to learn confidence signals that reflect

token-level reliability. As a result, the model struggles to identify where edits are needed, weakening the effectiveness of iterative refinement.

To formalize refinement-oriented diffusion models, we introduce the following definition.

Definition (Corrective Diffusion Language Model). A *Corrective Diffusion Language Model (CDLM)* is a masked diffusion language model that exhibits *corrective behavior*, namely error-aware refinement. Specifically, a CDLM:

1. assigns systematically lower confidence to erroneous or implausible tokens than to correct ones;
2. is able to leverage confidence signals to localize errors and iteratively improve sequence correctness under iterative refinement.

Together, these properties enable reliable error localization and targeted correction during diffusion-based refinement.

In the remainder of this section, we show that combining absorbing-mask corruption with uniform replacement corruption provides an effective and scalable mechanism for inducing corrective behavior. Absorbing corruption supports standard masked reconstruction, while uniform replacement introduces explicit noise at visible positions, requiring the model to detect and correct corrupted tokens. By mixing these two processes during training, the model can jointly learn reconstruction and error recognition, leading to stronger confidence calibration and more reliable refinement behavior.

6.1. Absorbing–Uniform Mixture Corruption

We corrupt a clean sequence $\mathbf{x} = (x_1, \dots, x_n)$ using a mixture of two complementary corruption processes: (1) absorbing-mask corruption, which removes tokens via masking and supports standard reconstruction, and (2) uniform replacement corruption, which injects visible but incorrect tokens. The corruption is applied sequentially in two stages.

Stage 1: Absorbing-mask corruption. We first sample a mask ratio $r_{\text{mask}} \sim \text{Uniform}(0, 1)$. For each position i , we draw a binary mask indicator

$$m_i \sim \text{Bernoulli}(r_{\text{mask}}),$$

yielding a partially masked sequence

$$x_i^{\text{mask}} = \begin{cases} \langle \text{mask} \rangle, & m_i = 1, \\ x_i, & m_i = 0. \end{cases}$$

Masked positions serve as standard denoising targets and receive reconstruction supervision.

Stage 2: Uniform replacement corruption. Uniform replacement noise is applied only to visible (unmasked) positions. For each position with $m_i = 0$, we sample $u_i \sim \text{Uniform}(0, 1)$ and mark it for replacement when

$$n_i = \begin{cases} 1, & u_i < \alpha, \\ 0, & \text{otherwise,} \end{cases}$$

where α controls the fraction of visible tokens corrupted by uniform noise. For positions with $n_i = 1$, the original token is replaced by a uniformly sampled token

$$t_i \sim \text{Uniform}(\mathcal{V} \setminus \{\langle \text{mask} \rangle, x_i\}),$$

which ensures that the replacement is visible and differs from the original clean token.

Final corrupted sequence. The final corrupted input \mathbf{x}_t is constructed as

$$x_{t,i} = \begin{cases} \langle \text{mask} \rangle, & m_i = 1, \\ t_i, & m_i = 0, n_i = 1, \\ x_i, & m_i = 0, n_i = 0. \end{cases}$$

Absorbing-mask corruption provides reconstruction supervision at masked positions, while uniform replacement introduces explicit noise at visible positions, requiring the model to recognize and downweight corrupted-but-unmasked tokens. Together, this mixture corruption supplies the supervision needed to jointly learn reconstruction and error awareness, enabling reliable error localization and targeted refinement.

6.2. Mixture Training Objective

Let \mathcal{M} denote the set of masked positions and \mathcal{N} the set of positions corrupted via uniform replacement. With per-token cross-entropy loss ℓ_i , we define the training objective as

$$\mathcal{L} = \frac{1}{|\mathcal{M}|} \sum_{i \in \mathcal{M}} \ell_i + \lambda_{\text{noise}} \cdot \frac{1}{|\mathcal{N}|} \sum_{i \in \mathcal{N}} \ell_i, \quad (1)$$

where λ_{noise} controls the relative weight of supervision on uniformly corrupted tokens.

The first term corresponds to standard masked reconstruction and preserves the model’s denoising capability, which is necessary for rewriting tokens during iterative refinement. The second term introduces explicit supervision on corrupted-but-visible tokens, requiring the model to recognize and downweight incorrect content. Together, these two terms train the model to both generate plausible replacements and identify which positions require editing. This supervision signal is absent in conventional masked diffusion training and is critical for inducing the error-aware

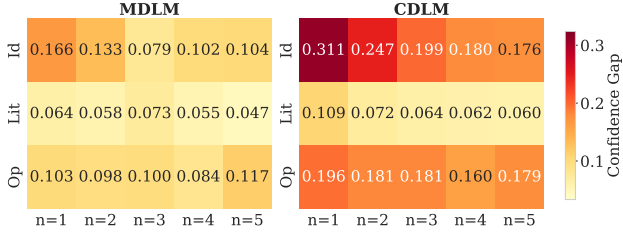


Figure 3. Confidence gap between clean and corrupted tokens for MDLM and CDLM across error types and numbers of replacements on the HumanEval dataset. Error types include identifier substitutions (Id), literal substitutions (Lit), and operator substitutions (Op). Larger values reflect stronger separation and improved error-awareness, with CDLM showing consistently higher gaps than MDLM.

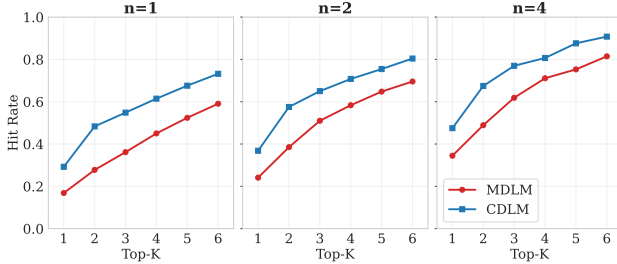


Figure 4. Top- K hit rate of identifying at least one true error among the K lowest-confidence positions for MDLM and CDLM on the HumanEval dataset. Higher values indicate more reliable error localization, with CDLM consistently outperforming MDLM across different numbers of corrupted tokens.

confidence and targeted refinement behavior characteristic of a CDLM.

We note that related work such as Generalized Interpolating Discrete Diffusion (GIDD) (von Rütte et al., 2025) also employs mixtures of absorbing noise and uniform noise corruption, and observes improved robustness and self-correction during generation. However, GIDD is primarily motivated by generalizing the diffusion framework and improving generation quality. In contrast, our work builds on the masked diffusion paradigm adopted by recent large diffusion language models such as LLaDA (Nie et al., 2025), and explicitly studies corrective behavior under iterative refinement. While masked diffusion decoding restricts updates to masked or remasked positions and treats other tokens as fixed conditioning context (see Algorithm 1 in Appendix B), GIDD’s sampling procedure implicitly updates all token positions through successive diffusion steps. This difference in update semantics enables localized, in-place editing in masked diffusion models, rather than holistic sequence updates.

7. Experiments

We evaluate the proposed absorbing–uniform mixture objective on CRB. Unless otherwise noted, our default model is CDLM-0.5B, obtained by finetuning the OPEN-DCODER-

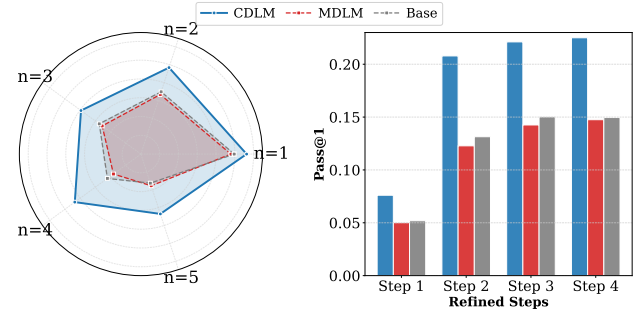


Figure 5. Pass@1 performance for MDLM, CDLM, and the base model under dynamic confidence-based refinement on the HumanEval dataset. Left: Pass@1 after four refinement steps with confidence threshold 0.9, shown across different numbers of corrupted tokens. Right: Mean Pass@1 averaged over all error types and corruption levels as the refinement depth increases. CDLM consistently outperforms MDLM and the base model under all settings.

Dataset	MDLM	CDLM	Base
HumanEval	0.157	0.257	0.168
HumanEval+	0.182	0.242	0.196
MBPP	0.114	0.175	0.114
MBPP+	0.137	0.226	0.120
Average	0.148	0.225	0.150

Table 3. Pass@1 on refinement-based code correction across standard coding benchmarks for MDLM, CDLM, and the base model. Scores are aggregated over all error types and corruption levels using four refinement steps with a confidence threshold of 0.9. CDLM consistently outperforms MDLM and the base model across datasets, demonstrating the benefit of explicit corrupted-token supervision for iterative refinement.

0.5B (Peng et al., 2025b) checkpoint for 2000 steps on the Nemotron coding corpus (NVIDIA et al., 2025). We compare three models throughout this section: (i) the pre-trained base model, (ii) the absorbing-only objective finetuned model, and (iii) the mixture-trained CDLM-0.5B. Training settings are identical across (ii) and (iii) except for the choice of objective.

7.1. How the Mixture Objective Improves Error Localization and Correction

We ablate the effect of training objective by comparing the absorbing-only model with the mixture-trained CDLM-0.5B. Both models use the same dataset, optimizer, learning rate schedule, and number of training steps. This isolates the effect of the mixture objective itself.

Error Localization Improvements. Error-token identification is evaluated using confidence gap and Top- K hit rate. Figure 3 reports the average confidence gap between clean and erroneous tokens across CRB difficulty levels. The mixture objective produces substantially larger gaps compared to both the base model and the absorbing-only

model, indicating that CDLM-0.5B assigns meaningfully lower confidence to incorrect tokens. Figure 4 reports the Top- K hit rate for $K \in \{1, \dots, 6\}$ across different numbers of corrupted tokens. Across all settings, CDLM consistently achieves higher hit rates than both the absorbing-only objective finetuned MDLM and the untrained base model. The advantage is particularly clear at small K , where correctly identifying at least one true error is most challenging. As K increases, the gap remains stable, indicating that the mixture objective produces confidence scores that more reliably prioritize erroneous tokens. Together, these results show that the mixture objective provides substantially improved token-level error localization.

Error Correction Improvements. We next evaluate end-to-end correction ability using deterministic Pass@1 under dynamic-confidence refinement. Figure 5 summarizes performance across corruption levels and refinement depths. In the left radar plot, each axis corresponds to a different corruption level $n_{\text{replace}} \in \{1, \dots, 5\}$, representing increasingly challenging error-correction scenarios. Across all difficulty levels, CDLM achieves consistently higher Pass@1 compared with both the absorbing-only objective finetuned MDLM and the untrained base model, indicating more reliable correction even when multiple errors must be revised.

The right panel of Figure 5 averages Pass@1 over all error types and corruption levels as the refinement depth increases. CDLM exhibits steady gains with each additional refinement step and maintains a consistent margin over the absorbing-only model.

Table 3 reports Pass@1 aggregated across all CRB settings. The mixture objective yields a substantial increase over absorbing-only finetuning as well as the unmodified base model, confirming that mixture training produces a significantly stronger correction capability.

7.2. Can CDLM Improve Pure Completion Performance?

We next examine whether the proposed mixture objective also benefits *pure completion* settings, in which the model is required to generate an entire program without any pre-existing errors or partially correct context. Specifically, the full body of the program (excluding the function signature) is replaced with mask tokens, and the model must generate the complete implementation from scratch. Unlike the correction setting, pure completion does not involve identifying or repairing injected errors, nor preserving any clean tokens. Instead, it evaluates general denoising and code generation ability under masked generation. For a controlled comparison, all models use the same remask-based decoding strategy: at each refinement step, a fixed number of low-confidence tokens are remasked according to a linear

schedule, and predictions are updated in subsequent iterations.

Table 4 reports Pass@1 and Pass@10 across HumanEval, HumanEval+, MBPP, and MBPP+. Across all benchmarks, the mixture objective improves both metrics relative to the absorbing-only finetuned model, indicating that incorporating uniform-noise supervision does not harm generation performance. Averaged across datasets, CDLM achieves higher Pass@1 and Pass@10 than both base model and the absorbing-only MDLM baseline. Compared with the untrained base model, CDLM attains comparable or better performance on most datasets. MBPP+ shows a small decrease relative to the base model, though the absorbing-only model performs even worse, suggesting that this deviation is dataset-specific rather than indicative of a systematic limitation.

We further evaluate both MDLM and CDLM under the ReMDM decoding strategy of Wang et al. (2025), which fixes token confidence at the step when each token is first unmasked. The overall trend remains unchanged: under both vanilla confidence-based decoding and ReMDM confidence, CDLM consistently outperforms MDLM, reinforcing that explicit supervision on corrupted tokens improves pure completion performance.

Overall, these results demonstrate that training with the mixture objective also improves pure completion performance under remask-based decoding strategy. CDLM consistently outperforms absorbing-only training across benchmarks. Intuitively, the mixture objective strengthens the model’s ability to recognize and revise implausible tokens during generation, enabling more reliable self-correction even when generating texts from scratch.

8. Sudoku: A Controlled From-Scratch Proxy for Pretraining

To study *corrective behavior* in diffusion language models under a fully controlled from-scratch regime, we train models on Sudoku from scratch. Sudoku is a compact symbolic domain in which the complete data distribution is observable and correctness is deterministically verifiable. This setting serves as a clean proxy for pretraining, where the model begins with no prior knowledge, corruption supplies the sole supervision signal, and learning dynamics are entirely dictated by the noising process.

Our Sudoku CDLM uses a Diffusion Transformer (DiT) architecture with approximately 37M parameters (12 layers, hidden size 512, 8 attention heads, MLP ratio 4, dropout 0.1), following the experimental setup of Kim et al. (2025). Each puzzle is represented as an 81-token sequence over a vocabulary of size 10 (a MASK token and digits 1–9). Training uses 36,000 puzzles, batch size 64, 200,000 optimi-

Training + Decoding	HumanEval		HumanEval+		MBPP		MBPP+		Avg	
	Pass@1	Pass@10								
MDLM (Vanilla)	0.190	0.384	0.170	0.341	0.106	0.312	0.177	0.449	0.161	0.372
CDLM (Vanilla)	0.216	0.415	0.205	0.390	0.131	0.352	0.207	0.472	0.190	0.407
Base (Vanilla)	0.188	0.366	0.167	0.317	0.157	0.350	0.231	0.502	0.186	0.384
MDLM (ReMDM)	0.198	0.384	0.172	0.341	0.108	0.328	0.170	0.444	0.162	0.374
CDLM (ReMDM)	0.212	0.427	0.200	0.378	0.141	0.350	0.211	0.476	0.191	0.408
Base (ReMDM)	0.182	0.329	0.164	0.293	0.160	0.366	0.232	0.485	0.185	0.368

Table 4. Pass@1 and Pass@10 on pure completion tasks across coding benchmarks. All evaluations use absorbing-mask reconstruction with a shared remask-based decoding framework. *Vanilla* decoding updates confidence at every refinement step, while *ReMDM* fixes each token’s confidence to the value it receives when first unmasked. Across both decoding strategies, the mixture objective (CDLM) consistently outperforms the absorbing objective(MDLM), indicating that corrupted-token supervision improves pure completion performance.

mization steps, learning rate 1×10^{-4} , weight decay 0.01, and a dynamically sampled masking ratio in [0.2, 0.9].

This controlled from-scratch environment allows us to isolate and evaluate two core aspects of corrective behavior: (i) whether training with the mixture objective induces error-awareness, namely the ability to assign lower confidence to corrupted tokens than to clean ones; and (ii) whether improved error localization translates into more effective iterative, in-place correction. In addition, we assess whether the mixture training objective improves standard absorbing-noise reconstruction, corresponding to pure denoising-based generation without uniform corruptions.

8.1. Uniform Noise Corruption: Error-Token Localization

We begin by evaluating whether the mixture objective induces error-aware confidence calibration under uniform noise corruption. Using a single forward pass without iterative refinement, a fraction of positions is corrupted by replacing the original digit with a uniformly sampled incorrect digit. We then measure the model’s confidence on clean versus corrupted positions. This setting isolates the effect of uniform-noise supervision on token-level confidence, independent of any iterative sampling dynamics.

Figure 6 reports confidence statistics across noise ratios of 0.1, 0.2, and 0.3. Models trained with the absorbing-only objective exhibit only weak separation between clean and corrupted digits. For example, at a noise ratio of 0.1, the ratio between mean confidence on clean digits and noisy digits is approximately $8.2\times$. In contrast, models trained with the mixture objective exhibit substantially stronger separation: the clean–noise confidence ratio exceeds $10,000\times$ at noise ratio 0.1 and remains above $160\times$ even at noise ratio 0.3.

These results show that mixture objective training induces strong error-awareness in the model’s confidence estimates. Corrupted digits are consistently assigned low confidence while clean digits retain high confidence, providing a reliable signal for error localization. This calibrated confidence

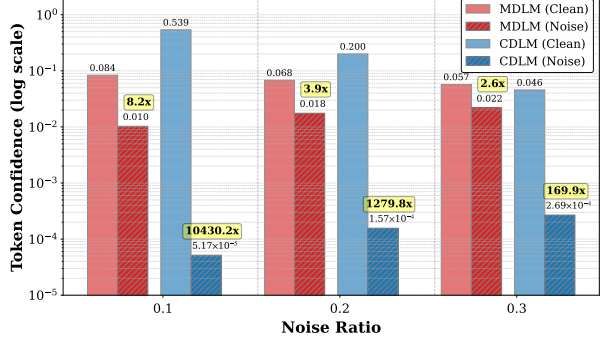


Figure 6. Confidence on clean and noisy digits under uniform corruption (log scale). We report clean–noise confidence ratios (yellow annotations) rather than absolute confidence gaps, since confidence values span multiple orders of magnitude in this setting. CDLM exhibits substantially larger clean–noise separation than MDLM across noise ratios, indicating significantly improved error localization compared with the absorbing-only objective.

forms a critical prerequisite for effective remask-based iterative correction, which we evaluate next.

8.2. Iterative Correction under Uniform Noise

We next study whether the improved error localization learned by CDLM translates into more effective iterative correction. Starting from grids corrupted by uniform noise, we define an editable region that always includes all noisy positions and may additionally include clean positions according to a specified editable ratio. Refinement is performed by iteratively remasking and resampling tokens within the editable region, while treating all other cells as fixed conditioning context. The full remask-based refinement procedure, including confidence computation and update rules, is detailed in Appendix C (Algorithm 2). We vary the noise ratio, the editable ratio, and the number of refinement steps, and evaluate board accuracy after the final refinement step.

Figure 7 summarizes results for two noise ratios (0.1 and 0.2), three editable ratios (0.4, 0.5, 0.6), and up to three refinement steps. Across all settings, CDLM consistently achieves higher board accuracy than MDLM. This advantage is already visible after a single refinement step and

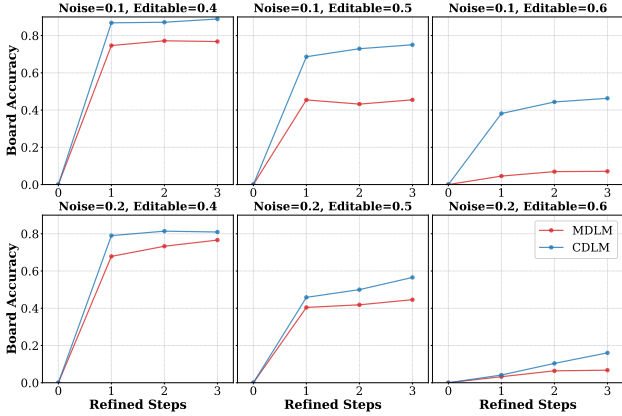


Figure 7. Sudoku board accuracy under uniform corruption with iterative diffusion sampling. Each subplot shows accuracy as a function of refinement steps for a specific combination of noise ratio and editable ratio. Across all difficulty settings, CDLM consistently achieves higher accuracy than MDLM.

often increases with additional steps. These results suggest that the improved confidence calibration learned by CDLM facilitates not only better error localization, but also more effective guided, in-place refinement under uniform corruption.

8.3. Pure Completion under Masked Denoising

We finally evaluate the effect of the mixture objective in a pure completion setting. Unlike the refinement experiments, this setup does not involve uniformly corrupted digits. Instead, a fraction of positions is replaced with a mask token, and the model performs multi-step denoising to produce a complete Sudoku grid using confidence-guided remask-based decoding. This setting corresponds to standard masked denoising and serves to assess whether training for corrective behavior also benefits pure denoising-based generation.

Figure 8 reports board accuracy across mask ratios from 0.3 to 0.6 using confidence-guided decoding with a threshold of 0.7. Models trained with the mixture objective consistently match or outperform those trained with the absorbing-only objective across all mask levels. The improvement is particularly pronounced at higher mask ratios, where confidence-guided refinement enables the model to identify and revise low-confidence digits during the denoising process. These results demonstrate that incorporating uniform-noise supervision not only preserves pure completion performance, but can also improve robustness in challenging masked reconstruction regimes.

9. Conclusion

We investigate corrective behavior in diffusion language models, with a particular focus on their ability to identify unreliable tokens in a complete sequence and iteratively

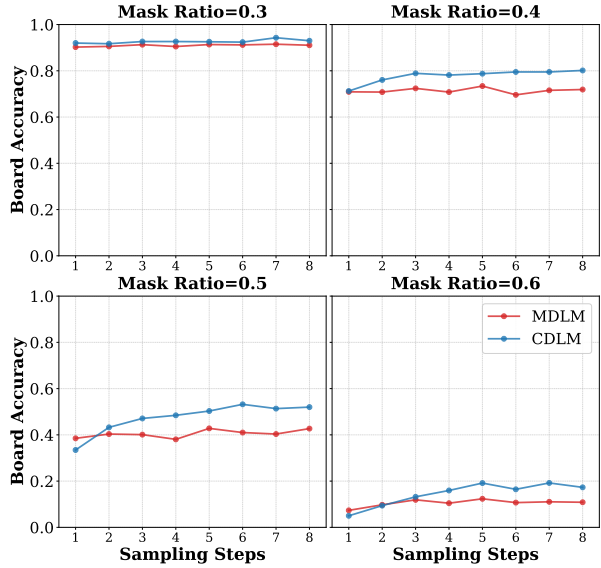


Figure 8. Pure completion performance under absorbing-mask corruption. Each subplot shows board accuracy as a function of sampling steps for a fixed mask ratio. Across all mask settings, CDLM matches or exceeds MDLM performance, indicating that the mixture objective does not introduce a tradeoff in reconstruction ability.

refine them while preserving correct content. To support systematic evaluation of this capability, we introduce the Code Revision Benchmark (CRB), a controllable and executable benchmark that isolates error localization and in-place correction from prefix-based generation. Using CRB and controlled synthetic environments, we demonstrate that standard masked diffusion objectives fail to induce error-aware, token-level confidence, which in turn leads to unreliable iterative refinement. To address this limitation, we propose a correction-oriented training principle based on a mixture of absorbing and uniform corruption that explicitly supervises visible corrupted tokens alongside masked reconstruction. Models trained with this objective consistently exhibit stronger error awareness, more reliable targeted refinement, and improved performance in both correction and pure completion settings, suggesting that confidence-aware diffusion training is a promising direction for enabling robust, in-place correction.

10. Limitations

Our goal is to isolate localized corrective behavior under masked diffusion and remask-based refinement, which aligns with the formulation commonly adopted by current foundation-model-style diffusion language models (Nie et al., 2025; Ye et al., 2025; Peng et al., 2025b). Accordingly, our study focuses on fixed-length correction settings, and the proposed Code Revision Benchmark (CRB) is designed to evaluate localized token replacement under preserved token alignment. As a result, CRB does not directly support

the evaluation of models that perform insertion or deletion operations, or more general variable-length editing, as explored in recent discrete diffusion formulations (Havasi et al., 2025; Chao et al., 2025; Zhang et al., 2025; Reid et al., 2023). Extending executable revision benchmarks to support variable-length editing and broader editing paradigms remains an interesting direction for future work.

References

Achiam, J., Adler, S., Agarwal, S., Ahmad, L., Akkaya, I., Aleman, F. L., Almeida, D., Altenschmidt, J., Altman, S., Anadkat, S., et al. Gpt-4 technical report. *arXiv preprint arXiv:2303.08774*, 2023.

Austin, J., Johnson, D. D., Ho, J., Tarlow, D., and van den Berg, R. Structured denoising diffusion models in discrete state-spaces. In Beygelzimer, A., Dauphin, Y., Liang, P., and Vaughan, J. W. (eds.), *Advances in Neural Information Processing Systems*, 2021a. URL <https://openreview.net/forum?id=h7-XixPCAL>.

Austin, J., Odena, A., Nye, M., Bosma, M., Michalewski, H., Dohan, D., Jiang, E., Cai, C. J., Terry, M., Le, Q. V., and Sutton, C. Program synthesis with large language models. *ArXiv*, abs/2108.07732, 2021b. URL <https://api.semanticscholar.org/CorpusID:237142385>.

Chao, C.-H., Sun, W.-F., Liang, H., Lee, C.-Y., and Krishnan, R. G. Beyond masked and unmasked: Discrete diffusion models via partial masking, 2025. URL <https://arxiv.org/abs/2505.18495>.

Chen, M., Tworek, J., Jun, H., Yuan, Q., de Oliveira Pinto, H. P., Kaplan, J., Edwards, H., Burda, Y., Joseph, N., Brockman, G., Ray, A., Puri, R., Krueger, G., Petrov, M., Khlaaf, H., Sastry, G., Mishkin, P., Chan, B., Gray, S., Ryder, N., Pavlov, M., Power, A., Kaiser, L., Bavarian, M., Winter, C., Tillet, P., Such, F. P., Cummings, D., Plappert, M., Chantzis, F., Barnes, E., Herbert-Voss, A., Guss, W. H., Nichol, A., Paino, A., Tezak, N., Tang, J., Babuschkin, I., Balaji, S., Jain, S., Saunders, W., Hesse, C., Carr, A. N., Leike, J., Achiam, J., Misra, V., Morikawa, E., Radford, A., Knight, M., Brundage, M., Murati, M., Mayer, K., Welinder, P., McGrew, B., Amodei, D., McCandlish, S., Sutskever, I., and Zaremba, W. Evaluating large language models trained on code, 2021. URL <https://arxiv.org/abs/2107.03374>.

Chen, S., Cong, K., and Li, J. Optimal inference schedules for masked diffusion models. *arXiv preprint arXiv:2511.04647*, 2025.

Chi, W., Chen, V., Shar, R., Mittal, A., Liang, J., Chiang, W.-L., Angelopoulos, A. N., Stoica, I., Neubig, G., Talwalkar, A., and Donahue, C. Edit-bench: Evaluating llm abilities to perform real-world instructed code edits, 2025. URL <https://arxiv.org/abs/2511.04486>.

Comanici, G., Bieber, E., Schaeckermann, M., Pasupat, I., Sachdeva, N., Dhillon, I., Blistein, M., Ram, O., Zhang, D., Rosen, E., et al. Gemini 2.5: Pushing the frontier with advanced reasoning, multimodality, long context, and next generation agentic capabilities. *arXiv preprint arXiv:2507.06261*, 2025.

Du, X., Liu, M., Wang, K., Wang, H., Liu, J., Chen, Y., Feng, J., Sha, C., Peng, X., and Lou, Y. Evaluating large language models in class-level code generation. In *2024 IEEE/ACM 46th International Conference on Software Engineering (ICSE)*, pp. 982–994, 2024. doi: 10.1145/3597503.3639219.

Grattafiori, A., Dubey, A., Jauhri, A., Pandey, A., Kadian, A., Al-Dahle, A., Letman, A., Mathur, A., Schelten, A., Vaughan, A., Yang, A., Fan, A., Goyal, A., Hartshorn, A., Yang, A., Mitra, A., Srivankumar, A., Korenev, A., Hinsvark, A., Rao, A., Zhang, A., Rodriguez, A., Gregerson, A., Spataru, A., Roziere, B., Biron, B., Tang, B., Chern, B., Caucheteux, C., Nayak, C., Bi, C., Marra, C., McConnell, C., Keller, C., Touret, C., Wu, C., Wong, C., Ferrer, C. C., Nikolaidis, C., Allonsius, D., Song, D., Pintz, D., Livshits, D., Wyatt, D., Esiobu, D., Choudhary, D., Mahajan, D., Garcia-Olano, D., Perino, D., Hupkes, D., Lakomkin, E., AlBadawy, E., Lobanova, E., Dinan, E., Smith, E. M., Radenovic, F., Guzmán, F., Zhang, F., Synnaeve, G., Lee, G., Anderson, G. L., Thattai, G., Nail, G., Mialon, G., Pang, G., Cucurell, G., Nguyen, H., Koverhaar, H., Xu, H., Touvron, H., Zarov, I., Ibarra, I. A., Kloumann, I., Misra, I., Evtimov, I., Zhang, J., Copet, J., Lee, J., Geffert, J., Vranes, J., Park, J., Mahadeokar, J., Shah, J., van der Linde, J., Billock, J., Hong, J., Lee, J., Fu, J., Chi, J., Huang, J., Liu, J., Wang, J., Yu, J., Bitton, J., Spisak, J., Park, J., Rocca, J., Johnstun, J., Saxe, J., Jia, J., Alwala, K. V., Prasad, K., Upasani, K., Plawiak, K., Li, K., Heafield, K., Stone, K., El-Arini, K., Iyer, K., Malik, K., Chiu, K., Bhalla, K., Lakhota, K., Rantala-Yearly, L., van der Maaten, L., Chen, L., Tan, L., Jenkins, L., Martin, L., Madaan, L., Malo, L., Blecher, L., Landzaat, L., de Oliveira, L., Muzzi, M., Pasupuleti, M., Singh, M., Paluri, M., Kardas, M., Tsimpoukelli, M., Oldham, M., Rita, M., Pavlova, M., Kambadur, M., Lewis, M., Si, M., Singh, M. K., Hassan, M., Goyal, N., Torabi, N., Bashlykov, N., Bogoychev, N., Chatterji, N., Zhang, N., Duchenne, O., Çelebi, O., Alrassy, P., Zhang, P., Li, P., Vasic, P., Weng, P., Bhargava, P., Dubal, P., Krishnan, P., Koura, P. S., Xu, P., He, Q., Dong, Q., Srinivasan, R., Ganapathy, R., Calderer, R., Cabral, R. S., Stojnic, R., Raileanu, R., Maheswari, R., Girdhar, R., Patel, R., Sauvestre, R., Polidoro, R., Sumbaly, R., Taylor, R., Silva,

R., Hou, R., Wang, R., Hosseini, S., Chennabasappa, S., Singh, S., Bell, S., Kim, S. S., Edunov, S., Nie, S., Narang, S., Raparthy, S., Shen, S., Wan, S., Bhosale, S., Zhang, S., Vandenhende, S., Batra, S., Whitman, S., Sootla, S., Collot, S., Gururangan, S., Borodinsky, S., Herman, T., Fowler, T., Sheasha, T., Georgiou, T., Scialom, T., Speckbacher, T., Mihaylov, T., Xiao, T., Karn, U., Goswami, V., Gupta, V., Ramanathan, V., Kerkez, V., Gonguet, V., Do, V., Vogeti, V., Albiero, V., Petrovic, V., Chu, W., Xiong, W., Fu, W., Meers, W., Martinet, X., Wang, X., Wang, X., Tan, X. E., Xia, X., Xie, X., Jia, X., Wang, X., Goldschlag, Y., Gaur, Y., Babaei, Y., Wen, Y., Song, Y., Zhang, Y., Li, Y., Mao, Y., Coudert, Z. D., Yan, Z., Chen, Z., Papakipos, Z., Singh, A., Srivastava, A., Jain, A., Kelsey, A., Shajnfeld, A., Gangidi, A., Victoria, A., Goldstand, A., Menon, A., Sharma, A., Boesenberg, A., Baevski, A., Feinstein, A., Kallet, A., Sangani, A., Teo, A., Yunus, A., Lupu, A., Alvarado, A., Caples, A., Gu, A., Ho, A., Poulton, A., Ryan, A., Ramchandani, A., Dong, A., Franco, A., Goyal, A., Saraf, A., Chowdhury, A., Gabriel, A., Bharambe, A., Eisenman, A., Yazdan, A., James, B., Maurer, B., Leonhardi, B., Huang, B., Loyd, B., Paola, B. D., Paranjape, B., Liu, B., Wu, B., Ni, B., Hancock, B., Wasti, B., Spence, B., Stojkovic, B., Gamido, B., Montalvo, B., Parker, C., Burton, C., Mejia, C., Liu, C., Wang, C., Kim, C., Zhou, C., Hu, C., Chu, C.-H., Cai, C., Tindal, C., Feichtenhofer, C., Gao, C., Civin, D., Beaty, D., Kreymer, D., Li, D., Adkins, D., Xu, D., Testuggine, D., David, D., Parikh, D., Liskovich, D., Foss, D., Wang, D., Le, D., Holland, D., Dowling, E., Jamil, E., Montgomery, E., Presani, E., Hahn, E., Wood, E., Le, E.-T., Brinkman, E., Arcaute, E., Dunbar, E., Smothers, E., Sun, F., Kreuk, F., Tian, F., Kokkinos, F., Ozgenel, F., Caggnioni, F., Kanayet, F., Seide, F., Florez, G. M., Schwarz, G., Badeer, G., Swee, G., Halpern, G., Herman, G., Sizov, G., Guangyi, Zhang, Lakshminarayanan, G., Inan, H., Shojanazeri, H., Zou, H., Wang, H., Zha, H., Habeeb, H., Rudolph, H., Suk, H., Aspegren, H., Goldman, H., Zhan, H., Damlaj, I., Molybog, I., Tufanov, I., Leontiadis, I., Veliche, I.-E., Gat, I., Weissman, J., Geboski, J., Kohli, J., Lam, J., Asher, J., Gaya, J.-B., Marcus, J., Tang, J., Chan, J., Zhen, J., Reizenstein, J., Teboul, J., Zhong, J., Jin, J., Yang, J., Cummings, J., Carvill, J., Shepard, J., McPhie, J., Torres, J., Ginsburg, J., Wang, J., Wu, K., U, K. H., Saxena, K., Khandelwal, K., Zand, K., Matosich, K., Veeraraghavan, K., Michelena, K., Li, K., Jagadeesh, K., Huang, K., Chawla, K., Huang, K., Chen, L., Garg, L., A, L., Silva, L., Bell, L., Zhang, L., Guo, L., Yu, L., Moshkovich, L., Wehrstedt, L., Khabsa, M., Avalani, M., Bhatt, M., Mankus, M., Hasson, M., Lennie, M., Reso, M., Groshev, M., Naumov, M., Lathi, M., Keneally, M., Liu, M., Seltzer, M. L., Valko, M., Restrepo, M., Patel, M., Vyatskov, M., Samvelyan, M., Clark, M., Macey, M., Wang, M., Hermoso, M. J., Metanat, M., Rastegari, M., Bansal, M., Santhanam, N., Parks, N., White, N., Bawa, N., Singhal, N., Egebo, N., Usunier, N., Mehta, N., Laptev, N. P., Dong, N., Cheng, N., Chernoguz, O., Hart, O., Salpekar, O., Kalinli, O., Kent, P., Parekh, P., Saab, P., Balaji, P., Rittner, P., Bontrager, P., Roux, P., Dollar, P., Zvyagina, P., Ratanchandani, P., Yuvraj, P., Liang, Q., Alao, R., Rodriguez, R., Ayub, R., Murthy, R., Nayani, R., Mitra, R., Parthasarathy, R., Li, R., Hogan, R., Battey, R., Wang, R., Howes, R., Rinott, R., Mehta, S., Siby, S., Bondu, S. J., Datta, S., Chugh, S., Hunt, S., Dhillon, S., Sidorov, S., Pan, S., Mahajan, S., Verma, S., Yamamoto, S., Ramaswamy, S., Lindsay, S., Lindsay, S., Feng, S., Lin, S., Zha, S. C., Patil, S., Shankar, S., Zhang, S., Zhang, S., Wang, S., Agarwal, S., Sajuyigbe, S., Chintala, S., Max, S., Chen, S., Kehoe, S., Satterfield, S., Govindaprasad, S., Gupta, S., Deng, S., Cho, S., Virk, S., Subramanian, S., Choudhury, S., Goldman, S., Remez, T., Glaser, T., Best, T., Koehler, T., Robinson, T., Li, T., Zhang, T., Matthews, T., Chou, T., Shaked, T., Vontimitta, V., Ajayi, V., Montanez, V., Mohan, V., Kumar, V. S., Mangla, V., Ionescu, V., Poenaru, V., Mihailescu, V. T., Ivanov, V., Li, W., Wang, W., Jiang, W., Bouaziz, W., Constable, W., Tang, X., Wu, X., Wang, X., Wu, X., Gao, X., Kleinman, Y., Chen, Y., Hu, Y., Jia, Y., Qi, Y., Li, Y., Zhang, Y., Zhang, Y., Adi, Y., Nam, Y., Yu, Wang, Zhao, Y., Hao, Y., Qian, Y., Li, Y., He, Y., Rait, Z., DeVito, Z., Rosnbrick, Z., Wen, Z., Yang, Z., Zhao, Z., and Ma, Z. The llama 3 herd of models, 2024. URL <https://arxiv.org/abs/2407.21783>.

Guo, D., Yang, D., Zhang, H., Song, J., Zhang, R., Xu, R., Zhu, Q., Ma, S., Wang, P., Bi, X., et al. Deepseek-r1: Incentivizing reasoning capability in llms via reinforcement learning. *arXiv preprint arXiv:2501.12948*, 2025a.

Guo, J., Li, Z., Liu, X., Ma, K., Zheng, T., Yu, Z., Pan, D., LI, Y., Liu, R., Wang, Y., Guo, S., Qu, X., Yue, X., Zhang, G., Chen, W., and Fu, J. Codeeditor-bench: Evaluating code editing capability of LLMs. In *ICLR 2025 Third Workshop on Deep Learning for Code*, 2025b. URL <https://openreview.net/forum?id=6yTgoh0J0X>.

Havasi, M., Karrer, B., Gat, I., and Chen, R. T. Q. Edit flows: Variable length discrete flow matching with sequence-level edit operations. In *The Thirty-ninth Annual Conference on Neural Information Processing Systems*, 2025. URL <https://openreview.net/forum?id=FXWwYz1p8a>.

He, Z., Sun, T., Tang, Q., Wang, K., Huang, X., and Qiu, X. DiffusionBERT: Improving generative masked language models with diffusion models. In Rogers, A., Boyd-Graber, J., and Okazaki, N. (eds.), *Proceedings of the 61st Annual Meeting of the Association for Computational Linguistics (Volume 1: Long Papers)*, pp. 4521–

4534, Toronto, Canada, July 2023. Association for Computational Linguistics. doi: 10.18653/v1/2023.acl-long.248. URL <https://aclanthology.org/2023.acl-long.248/>.

Huang, J., Chen, X., Mishra, S., Zheng, H. S., Yu, A. W., Song, X., and Zhou, D. Large language models cannot self-correct reasoning yet. In *The Twelfth International Conference on Learning Representations*, 2024. URL <https://openreview.net/forum?id=1kmD3fKBPQ>.

Jimenez, C. E., Yang, J., Wettig, A., Yao, S., Pei, K., Press, O., and Narasimhan, K. Swe-bench: Can language models resolve real-world github issues?, 2024. URL <https://arxiv.org/abs/2310.06770>.

Kang, W., Galim, K., Oh, S., Lee, M., Zeng, Y., Zhang, S., Hooper, C., Hu, Y., Koo, H. I., Cho, N. I., et al. Parallel-bench: Understanding the trade-offs of parallel decoding in diffusion llms. *arXiv preprint arXiv:2510.04767*, 2025.

Kim, J., Kim, S., Lee, T., Pan, D. Z., Kim, H., Kakade, S., and Chen, S. Fine-tuning masked diffusion for provable self-correction, 2025. URL <https://arxiv.org/abs/2510.01384>.

Kitanidis, E. and Hunter, C. J. pydra: Probing code representations with synthetic clones and bugs. In *NeurIPS 2025 Fourth Workshop on Deep Learning for Code*, 2025.

Labs, I., Khanna, S., Kharbanda, S., Li, S., Varma, H., Wang, E., Birnbaum, S., Luo, Z., Miraoui, Y., Palrecha, A., Ermon, S., Grover, A., and Kuleshov, V. Mercury: Ultra-fast language models based on diffusion, 2025. URL <https://arxiv.org/abs/2506.17298>.

Lee, S., Kim, S., Kim, S., Park, J., and Park, D. Effective test-time scaling of discrete diffusion through iterative refinement. *arXiv preprint arXiv:2511.05562*, 2025a.

Lee, Y.-J., Kim, S., Lee, B.-K., Moon, M., Hwang, Y., Kim, J. M., Neubig, G., Welleck, S., and Choi, H.-J. Refinebench: Evaluating refinement capability of language models via checklists, 2025b. URL <https://arxiv.org/abs/2511.22173>.

Li, X. L., Thickstun, J., Gulrajani, I., Liang, P., and Hashimoto, T. Diffusion-LM improves controllable text generation. In Oh, A. H., Agarwal, A., Belgrave, D., and Cho, K. (eds.), *Advances in Neural Information Processing Systems*, 2022. URL <https://openreview.net/forum?id=3s9IrEsjLyk>.

Liu, J., Xia, C. S., Wang, Y., and ZHANG, L. Is your code generated by chatgpt really correct? rigorous evaluation of large language models for code generation. In Oh, A., Naumann, T., Globerson, A., Saenko, K., Hardt, M., and Levine, S. (eds.), *Advances in Neural Information Processing Systems*, volume 36, pp. 21558–21572. Curran Associates, Inc., 2023a.

Liu, J., Xia, C. S., Wang, Y., and ZHANG, L. Is your code generated by chatGPT really correct? rigorous evaluation of large language models for code generation. In *Thirty-seventh Conference on Neural Information Processing Systems*, 2023b. URL <https://openreview.net/forum?id=1qvx610Cu7>.

Ni, J., Liu, Q., Du, C., Dou, L., Yan, H., Wang, Z., Pang, T., and Shieh, M. Q. Training optimal large diffusion language models, 2025. URL <https://arxiv.org/abs/2510.03280>.

Nie, S., Zhu, F., You, Z., Zhang, X., Ou, J., Hu, J., Zhou, J., Lin, Y., Wen, J.-R., and Li, C. Large language diffusion models, 2025. URL <https://arxiv.org/abs/2502.09992>.

NVIDIA, :, Basant, A., Khairnar, A., Paithankar, A., Khattar, A., Renduchintala, A., Malte, A., Bercovich, A., Hazare, A., Rico, A., Ficek, A., Kondratenko, A., Shaposhnikov, A., Bukharin, A., Taghibakhshi, A., Barton, A., Maha-baleshwarkar, A. S., Shen, A., Tao, A., Guan, A., Shors, A., Mandarwal, A., Mehta, A., Venkatesan, A., Sharabi, A., Aithal, A., Poojary, A., Dattagupta, A., Bud-dharaju, B., Zhu, B., Simkin, B., Kartal, B., Rouhani, B. D., Chen, B., Ginsburg, B., Norick, B., Yu, B., Catan-zaro, B., Wang, C., Truong, C., Mungekar, C., Patel, C., Alexiuk, C., Munley, C., Parisien, C., Su, D., Afrimi, D., Korzekwa, D., Rohrer, D., Gitman, D., Mosallanezhad, D., Narayanan, D., Rekesh, D., Yared, D., Pykhtar, D., Ahn, D., Riach, D., Long, E., Ning, E., Chung, E., Galinkin, E., Bakhturina, E., Prasad, G., Shen, G., Qian, H., Elisha, H., Sharma, H., Ross, H., Ngo, H., Sahota, H., Wang, H., Shin, H. C., Huang, H., Cunningham, I., Gitman, I., Moshkov, I., Jung, J., Kautz, J., Scowcroft, J. P., Casper, J., Zhang, J., Zeng, J., Zhang, J., Xue, J., Huang, J., Conway, J., Kamalu, J., Cohen, J., Jennings, J., Vialard, J. V., Yi, J., Parmar, J., Briski, K., Cheung, K., Luna, K., Wyss, K., Santhanam, K., Kong, K., Pawelec, K., Anik, K., Li, K., Ahmadian, K., McAfee, L., Sleiman, L., Der-czynski, L., Vega, L., de Melo, M. R., Sreedhar, M. N., Chochowski, M., Cai, M., Kliegl, M., Stepniewska-Dziubinska, M., Novikov, M., Samadi, M., Price, M., Boubdir, M., Boone, M., Evans, M., Bien, M., Zawal-ski, M., Martinez, M., Chrzanowski, M., Shoeybi, M., Patwary, M., Dhameja, N., Assaf, N., Habibi, N., Bhatia, N., Pope, N., Tajbakhsh, N., Juluru, N. K., Rybakov, O., Hrinchuk, O., Kuchaiev, O., Olabiyi, O., Ribalta, P., Subramanian, P., Chadha, P., Molchanov, P., Dykas, P., Jin, P., Bialecki, P., Januszewski, P., Thalasta, P., Gaikwad, P., Varshney, P., Gundecha, P., Tredak, P., Mahabadi, R. K.,

Patel, R., El-Yaniv, R., Rajan, R., Cheruvu, R., Shahbazyani, R., Borkar, R., Gala, R., Waleffe, R., Zhang, R., Hewett, R. J., Prenger, R., Jain, S., Kriman, S., Satheesh, S., Kaji, S., Yurick, S., Muralidharan, S., Narenthiran, S., Bak, S., Sameni, S., Han, S., Ramasamy, S., Ghosh, S., Sreenivas, S. T., Thomas, S., Diao, S., Gopal, S., Prabhumoye, S., Toshniwal, S., Ding, S., Singh, S., Jain, S., Majumdar, S., Singhal, S., Alborghetti, S., Akter, S. N., Kong, T., Moon, T., Hliwiak, T., Asida, T., Wang, T., Konuk, T., Vashishth, T., Poon, T., Karpas, U., Noroozi, V., Srinivasan, V., Korthikanti, V., Fugro, V., Kalluru, V., Kurin, V., Lavrukhin, V., Ahmad, W. U., Du, W., Byeon, W., Lu, X., Dong, X., Karnati, Y., Choi, Y., Zhang, Y., Lin, Y., Fu, Y., Suhara, Y., Dong, Z., Li, Z., Zhu, Z., and Chen, Z. Nvidia nemotron nano 2: An accurate and efficient hybrid mamba-transformer reasoning model, 2025. URL <https://arxiv.org/abs/2508.14444>.

Opu, M. N. I., Wang, S., and Chowdhury, S. Llm-based detection of tangled code changes for higher-quality method-level bug datasets. *arXiv preprint arXiv:2505.08263*, 2025.

Peng, F. Z., Bezemek, Z., Patel, S., Rector-Brooks, J., Yao, S., Tong, A., and Chatterjee, P. Path planning for masked diffusion models with applications to biological sequence generation. In *ICLR 2025 Workshop on Deep Generative Model in Machine Learning: Theory, Principle and Efficacy*, 2025a. URL <https://openreview.net/forum?id=fFuVPKpSt0>.

Peng, F. Z., Zhang, S., Tong, A., and Open-dLLM Contributors. Open-dLLM: Open diffusion large language models, 2025b. URL <https://github.com/pengzhangzhi/Open-dLLM>.

Reid, M., Hellendoorn, V. J., and Neubig, G. DiffusER: Diffusion via edit-based reconstruction. In *The Eleventh International Conference on Learning Representations*, 2023. URL <https://openreview.net/forum?id=nG9RF9z1yy3>.

Sahoo, S. S., Arriola, M., Gokaslan, A., Marroquin, E. M., Rush, A. M., Schiff, Y., Chiu, J. T., and Kuleshov, V. Simple and effective masked diffusion language models. In *The Thirty-eighth Annual Conference on Neural Information Processing Systems*, 2024. URL <https://openreview.net/forum?id=L4uaAR4ArM>.

Schiff, Y., Sahoo, S. S., Phung, H., Wang, G., Boshar, S., Dalla-torre, H., de Almeida, B. P., Rush, A. M., PIERROT, T., and Kuleshov, V. Simple guidance mechanisms for discrete diffusion models. In *The Thirteenth International Conference on Learning Representations*, 2025. URL <https://openreview.net/forum?id=i5MrJ6gG1>.

Song, Y., Zhang, Z., Luo, C., Gao, P., Xia, F., Luo, H., Li, Z., Yang, Y., Yu, H., Qu, X., Fu, Y., Su, J., Zhang, G., Huang, W., Wang, M., Yan, L., Jia, X., Liu, J., Ma, W.-Y., Zhang, Y.-Q., Wu, Y., and Zhou, H. Seed diffusion: A large-scale diffusion language model with high-speed inference, 2025. URL <https://arxiv.org/abs/2508.02193>.

Tang, Z., Li, Z., Xiao, Z., Ding, T., Sun, R., Wang, B., Liu, D., Huang, F., Liu, T., Yu, B., and Lin, J. Realcritic: Towards effectiveness-driven evaluation of language model critiques. *arXiv preprint arXiv:2501.14492*, 2024.

von Rütte, D., Fluri, J., Ding, Y., Orvieto, A., Schölkopf, B., and Hofmann, T. Generalized interpolating discrete diffusion. In *Forty-second International Conference on Machine Learning*, 2025. URL <https://openreview.net/forum?id=rvZv7sDPV9>.

Wang, G., Schiff, Y., Sahoo, S. S., and Kuleshov, V. Remasking discrete diffusion models with inference-time scaling. In *The Thirty-ninth Annual Conference on Neural Information Processing Systems*, 2025. URL <https://openreview.net/forum?id=IJryQAoy0p>.

Wang, Y. and Zhao, Y. Rupbench: Benchmarking reasoning under perturbations for robustness evaluation in large language models, 2024. URL <https://arxiv.org/abs/2406.11020>.

Widyasari, R., Sim, S. Q., Lok, C., Qi, H., Phan, J., Tay, Q., Tan, C., Wee, F., Tan, J. E., Yieh, Y., et al. Bugsinpy: a database of existing bugs in python programs to enable controlled testing and debugging studies. In *Proceedings of the 28th ACM joint meeting on european software engineering conference and symposium on the foundations of software engineering*, pp. 1556–1560, 2020.

Xu, Z. and Sheng, V. S. Lecprompt: A prompt-based approach for logical error correction with codebert, 2024. URL <https://arxiv.org/abs/2410.08241>.

Yang, A., Li, A., Yang, B., Zhang, B., Hui, B., Zheng, B., Yu, B., Gao, C., Huang, C., Lv, C., Zheng, C., Liu, D., Zhou, F., Huang, F., Hu, F., Ge, H., Wei, H., Lin, H., Tang, J., Yang, J., Tu, J., Zhang, J., Yang, J., Yang, J., Zhou, J., Zhou, J., Lin, J., Dang, K., Bao, K., Yang, K., Yu, L., Deng, L., Li, M., Xue, M., Li, M., Zhang, P., Wang, P., Zhu, Q., Men, R., Gao, R., Liu, S., Luo, S., Li, T., Tang, T., Yin, W., Ren, X., Wang, X., Zhang, X., Ren, X., Fan, Y., Su, Y., Zhang, Y., Zhang, Y., Wan, Y., Liu, Y., Wang, Z., Cui, Z., Zhang, Z., Zhou, Z., and Qiu, Z. Qwen3 technical report, 2025. URL <https://arxiv.org/abs/2505.09388>.

Ye, J., Xie, Z., Zheng, L., Gao, J., Wu, Z., Jiang, X., Li, Z., and Kong, L. Dream 7b: Diffusion large language mod-

els, 2025. URL <https://arxiv.org/abs/2508.15487>.

Zhang, A., Sivakumar, A., Tang, C.-W., and Thomas, C. Flexible-length text infilling for discrete diffusion models. In Christodoulopoulos, C., Chakraborty, T., Rose, C., and Peng, V. (eds.), *Proceedings of the 2025 Conference on Empirical Methods in Natural Language Processing*, pp. 31332–31347, Suzhou, China, November 2025. Association for Computational Linguistics. ISBN 979-8-89176-332-6. doi: 10.18653/v1/2025.emnlp-main.1597. URL <https://aclanthology.org/2025.emnlp-main.1597/>.

Zhu, F., You, Z., Xing, Y., Huang, Z., Liu, L., Zhuang, Y., Lu, G., Wang, K., Wang, X., Wei, L., Guo, H., Hu, J., Ye, W., Chen, T., Li, C., Tang, C., Feng, H., Hu, J., Zhou, J., Zhang, X., Lan, Z., Zhao, J., Zheng, D., Li, C., Li, J., and Wen, J.-R. Llada-moe: A sparse moe diffusion language model, 2025. URL <https://arxiv.org/abs/2509.24389>.

Contents of the Appendix

The following contents are included in the appendix:

- Sec. A discusses related work on self-correction and refinement in large language models.
- Sec. B presents the remask-based iterative refinement procedure.
- Sec. C studies remask-based iterative refinement for Sudoku under uniform noise.

A. Related Work on Self-Correction and Refinement in Large Language Models

A number of prior studies on large language models have explored concepts related to correction and refinement across general datasets and multiple domains, often under the formulation of self-correction, critique, or iterative improvement. Huang et al. (2024) study models’ ability to self-correct on reasoning-oriented benchmarks, focusing on improving final answers through iterative reasoning. RealCritic (Tang et al., 2024) proposes a critique-and-correction framework that explicitly models how the quality of critiques affects downstream solution refinement, while RefineBench (Lee et al., 2025b) allows models to autonomously decide whether refinement is necessary and to generate self-feedback before revision. In task-specific settings, particularly for code, several benchmarks have been proposed to evaluate code editing and repair capabilities under more realistic scenarios. Tangled Code Changes (Opu et al., 2025), BugsInPy (Widyasari et al., 2020), and Pydra (Kitanidis & Hunter, 2025) construct benchmarks based on real or synthetic bugs to evaluate code correction capabilities. More recent benchmarks such as CodeEditorBench (Guo et al., 2025b), SWE-Bench (Jimenez et al., 2024), and EditBench (Chi et al., 2025) further study code editing in realistic development settings, often requiring models to perform multi-line, instruction-driven, or repository-level modifications.

While these benchmarks demonstrate that language models can revise and improve their outputs under various correction paradigms, they predominantly treat correction as a task-level or procedural process that generates revised solutions from scratch or through external critique loops. In particular, refinement in these settings is typically not performed *in place* on a complete input, but instead relies on regeneration, multi-stage prompting, or auxiliary feedback mechanisms. In contrast, our Code Revision Benchmark (CRB) isolates *in-place refinement* by applying localized corruptions to a complete input and evaluating whether a model can identify and correct erroneous tokens while preserving correct context.

B. Remask-Based Iterative Refinement Procedure

Algorithm 1 summarizes the confidence-based iterative refinement procedure used throughout our experiments. At each step, low-confidence tokens are explicitly remasked and resampled, while all other tokens are treated as fixed conditioning context. Unlike GIDD (von Rütte et al., 2025), which performs holistic diffusion updates over all token positions and does not employ an explicit remasking mechanism, this procedure explicitly restricts updates to masked or remasked positions, enabling localized, in-place refinement.

C. Remask-Based Iterative Refinement for Sudoku under Uniform Noise

We consider Sudoku boards represented as sequences of length 81, where each token takes values from a discrete vocabulary $\mathcal{V} = \{\langle \text{mask} \rangle, 1, \dots, 9\}$. Given an initial grid corrupted by uniform replacement noise, we define an *editable set* of token positions $\mathcal{E} \subseteq \{1, \dots, 81\}$. By construction, \mathcal{E} always contains all uniformly corrupted (noisy) positions, and may additionally include a subset of clean positions according to a specified editable ratio.

Notes. The editable set \mathcal{E} is fixed throughout decoding and is constructed *a priori* for controlled evaluation. The remasking set $\mathcal{R}^{(t)}$ is recomputed at every step based on token-level confidence, but is always restricted to \mathcal{E} . As a result, the procedure performs localized, in-place correction by allowing updates only within the editable region, while preserving the remainder of the grid as immutable conditioning context.

Algorithm 1 Confidence-Based Iterative Refinement with Remasking

Input: Initial sequence $\mathbf{z}^{(0)} \in (\mathcal{V} \cup \{\langle \text{mask} \rangle\})^n$;
 Denoising model $p_\theta(\cdot | \cdot)$;
 Confidence threshold $\tau \in (0, 1)$;
 Number of refinement steps T
Output: Refined sequence $\mathbf{z}^{(T)}$

for $t = 0, 1, \dots, T - 1$ **do**

// Parallel denoising prediction

Compute token distributions $p_\theta(\cdot | \mathbf{z}^{(t)})$ for all positions Compute confidences $c_i^{(t)} = \max_{v \in \mathcal{V}} p_\theta(v | \mathbf{z}^{(t)})$ for all i
 Compute predictions

$$\hat{x}_i^{(t)} = \begin{cases} \arg \max_{v \in \mathcal{V}} p_\theta(v | \mathbf{z}^{(t)}), & z_i^{(t)} = \langle \text{mask} \rangle \\ z_i^{(t)}, & \text{otherwise} \end{cases} \quad \text{for all } i$$

// Identify low-confidence positions

$$r^{(t)} \leftarrow \{i \in \{1, \dots, n\} \mid c_i^{(t)} < \tau\}$$

// Remasking and update

foreach $i = 1, \dots, n$ **do**

$$z_i^{(t+1)} \leftarrow \begin{cases} \langle \text{mask} \rangle, & i \in r^{(t)} \\ \hat{x}_i^{(t)}, & \text{otherwise} \end{cases}$$

return $\mathbf{z}^{(T)}$

Algorithm 2 Remask-Based Iterative Refinement with Editable Tokens (Sudoku)

Input: Initial sequence $\mathbf{z}^{(0)} = (z_1^{(0)}, \dots, z_{81}^{(0)}), z_i^{(0)} \in \mathcal{V} = \{\langle \text{mask} \rangle, 1, \dots, 9\}$, corrupted by uniform replacement noise;
 Denoising model $p_\theta(\cdot | \cdot)$;
 Editable token set $\mathcal{E} \subseteq \{1, \dots, 81\}$ containing all noisy positions;
 Confidence threshold τ ;
 Number of refinement steps T .
Output: Refined sequence $\mathbf{z}^{(T)}$.

for $t = 0, 1, \dots, T - 1$ **do**

// Denoising prediction (token predictions and confidence)

for $i = 1, 2, \dots, 81$ **do**

Compute $p_\theta(\cdot | \mathbf{z}^{(t)})$ at position i ;

$$\hat{x}_i^{(t)} \leftarrow \arg \max_{v \in \mathcal{V} \setminus \{\langle \text{mask} \rangle\}} p_\theta(v | \mathbf{z}^{(t)});$$

$$c_i^{(t)} \leftarrow \max_{v \in \mathcal{V} \setminus \{\langle \text{mask} \rangle\}} p_\theta(v | \mathbf{z}^{(t)}).$$

// Identify remasking set (restricted to editable tokens)

$$\mathcal{R}^{(t)} \leftarrow \{i \in \mathcal{E} : c_i^{(t)} < \tau\};$$

// Construct next iterate; non-editable tokens remain fixed

for $i = 1, 2, \dots, 81$ **do**

if $i \in \mathcal{R}^{(t)}$ **then**

$$z_i^{(t+1)} \leftarrow \langle \text{mask} \rangle;$$

else

if $i \in \mathcal{E}$ **then**

$$z_i^{(t+1)} \leftarrow \hat{x}_i^{(t)};$$

else

$$z_i^{(t+1)} \leftarrow z_i^{(t)}; ;$$

// Non-editable tokens remain unchanged

return $\mathbf{z}^{(T)}$
